EUROPEAN ROTORCRAFT FORUM 2017: 717

CONCEPTUAL AND PRELIMINARY DESIGN OF A HYBRID DUST FILTER FOR HELICOPTER ENGINES

Nicholas Bojdo & Antonio Filippone
University of Manchester

Abstract

We present our ongoing work in the field of helicopter engine protection. Recent sand ingestion-related aircraft crash mishaps have highlighted the inadequacy of some particle separator types to remove the finest particles from the engine inlet air, which melt more readily and are potentially more hazardous to operation that the larger, erosive quartz particles that are successfully removed. Inertia-based separators such as integrated particle separators on the T700 and RTM322 military helicopter engines, or the externally-mounted vortex tube panels are unable to separate well particles below 10 microns in size, yet the former is small and compact and the latter exhibits a low pressure loss compared to the high separation efficiency barrier filter separator. In the current work we examine these competing cost functions and present a new metric trade-off designs at the concept stage. We use this metric to demonstrate why vortex tubes may be the superior technology for ISO Coarse test dust, but barrier filters succeed for a finer, more realistic test dust called AFRL 02. Finally we propose a hybrid concept that combines the benefits of two particle separator concepts to remove a greater proportion of dust than either of the two contributory devices can do alone.

1. INTRODUCTION

Particle filters or separators are fitted to the air intakes of helicopter power plants to remove sand, dust and other foreign objects from the air. They are numerous in form, making use of a particle's inertia or diameter to remove it from an air streamline. They have been commonplace on helicopters since the late 70s when the T700 engine program featuring the first integrated inertial particle separator was launched. Up to then, unprotected engines were lasting as little as 25 hours in desert conditions [1].

While the introduction of particle separators dramatically improved engine life on the test bed, the reality of operation in operations such as Desert Shield/Storm revealed logistical problems and a large difference in separator performance. Part of the issue is the difference in composition between the test dust and the real operation dust. Particle separators and filters are qualified with ISO Coarse test dust, a dust of 78% quartz with a mean particle size of 38 microns. The bulk inertia of such dust is greater than that of the reality: a collection of finer particles of often much less dense clays and silts. The consequence of this is an over prediction of the separator's ability to remove potentially harmful particulate [2], and unanticipated damage such as deposition on nozzle guide vanes [3].

The damage caused by ingested particulate is well documented (see Ref. [4]). The damage may be *gradual*, creating an increased cost-of-ownership problem through increased fuel burn and loss of useful power, or more *instant* through engine surge. The latter occurs if the rate of deposition of molten dust is great enough to block the nozzle guide vanes passages, or the compressor erosion is severe enough to significantly shift the surge line.

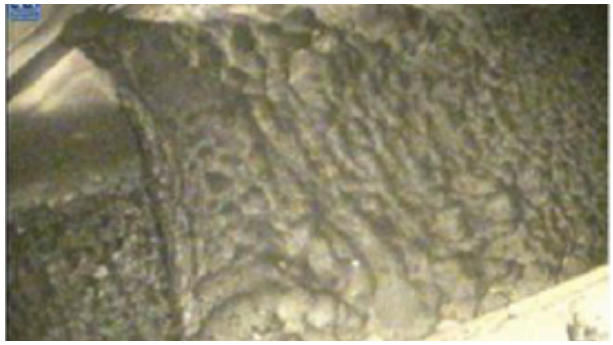

Figure 1: Turbine vane blades of MV22 written off after hard landing and fire at Creech AFB, Nevada, shows the glasslike accretion of melted particles [5].

The fatal crash landing of an MV-22 Osprey in May 2015 may have been caused by sand ingestion, according to some reports [5]. Returning to base on Oahu Island, Hawaii, the MV-22 entered three successive brownout clouds after two aborted landings. At less than two rotor disks above the ground, the left engine suffered a flame out. Lacking sufficient power for the hover, the aircraft dropped

to the ground, killing two marines on board. Subsequent inspection of the teardown revealed significant deposited material on the first stage NGVs (see Figure 1), known as CMAS glass (calcium-alumina-magnesium-silicate) [5]. While CMAS can cause long-term through hot corrosion of thermal barrier coating, the surge in this case was thought to be due to rapid loss of turbine capacity.

The significance of the MV-22 crash is that the engine that failed was fitted with an inertial particle separator (IPS) [5]. Studies in the literature show a drop off in IPS separation efficiency when particle diameter drops below 20 microns. This added to the fact that the mineralogy of the dust on Hawaii is likely to have high glass content may go some way to explain why the IPS was ineffective in this environment.

The failure of the system prompted the commissioning of a replacement Engine Inlet Barrier Filter (EIBF) solution for the V-22 intake, as described in Ref. [6] and shown in Figure 2. The EIBF stops particles by trapping them between its layers of pleated fabric. However, as elaborated by Bojdo [7], the pressure loss across the IBF can be substantial at high engine mass flow rates, and worsens with time as more particles are captured. Contrast this with the inertial type separators, which eject centrifuged particles overboard via a scavenge channel. However, the EIBF achieves a much higher separation efficiency than the inertial type separators [8], hence its inclusion in the new system in Figure 2.

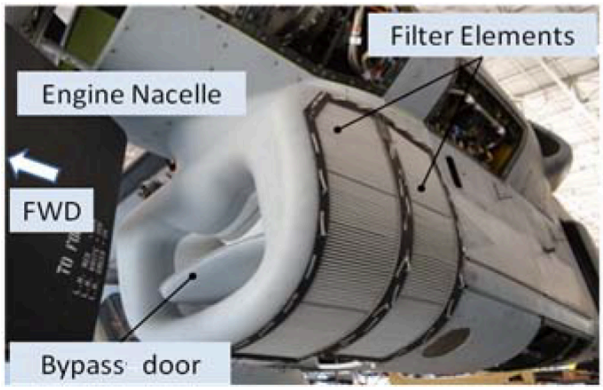

Figure 2: Engine Inlet Barrier Filter solution for the V-22 [6].

The success of the EIBF is yet to be seen. The solution presented in Figure 2 shows a very large filtration surface area. This adds extra weight, volume, and complexity to the intake system, and is one of the main reasons why inertial systems are preferred for larger volume engines. The EIBF must also be regularly cleaned. The IPS, conversely, is much more compact and requires little maintenance. This is one example of a trade-off in particle separator design. In the current work we discuss these trade-offs, and propose a new hybrid separator that aims to combine the best features of two separator types.

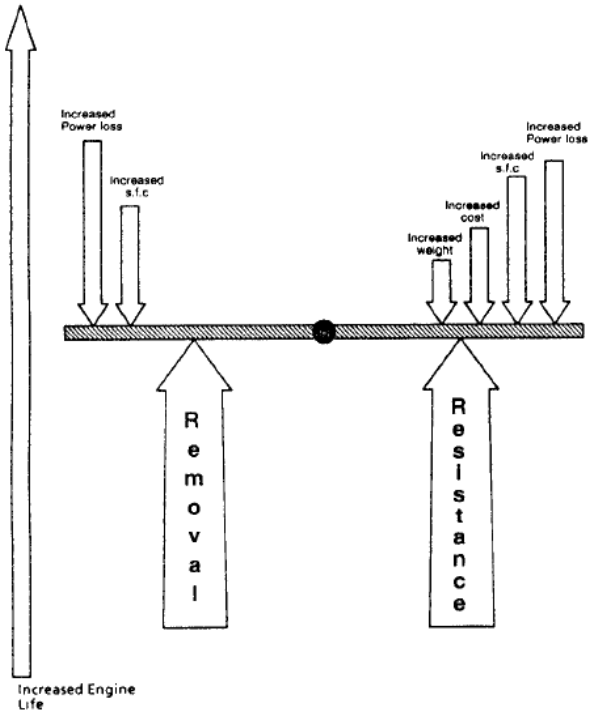

Figure 3: Removal vs. Resistance [3].

2. BACKGROUND

2.1. Design Process

Designing a system to protect helicopter engines is a balance between removal and resistance. No system is able to remove all contaminants from the inlet air without some loss of engine performance, therefore the designer must weigh the extension of engine life against the loss in lifting capacity or additional fuel burn. Protection encompasses internal (e.g. coatings) and external solutions (e.g. inlet particle separators). Internal solutions are focused on *resisting* the damage when particle interact with engine components, while external solutions focus on *removing* the particles. Together they combine to increase engine life, but not without

some competing costs. For example, both solutions increase specific fuel consumption (SFC). The level of acceptable SFC loss may be fixed by design requirements; the system designer must decide on what proportion is given away to resistance, and what proportion is given away to removal. This is depicted in Figure 3, presented by Mann & Warnes [3].

In addition to SFC, one may also consider power loss as a cost function when designing a protection system. In fact, there are a number of other potential cost functions, such as added weight, cost, volume and maintainability. As discussed, there are many concepts available, all of which will behave differently with respect to these cost functions. The contribution by Mann & Warnes describes the formalized procedure used by Rolls-Royce to rank candidate designs, shown in Figure 4 [3]. Performance parameters that impact on the cost functions such as pressure loss, separation efficiency etc. are used as selection criteria. The relative weighting of these are decided by customer requirements, then each candidate design is scored against the criteria, either by analysis or expert panel.

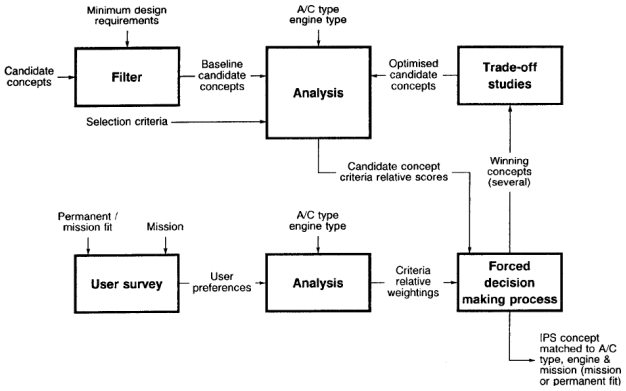

Figure 4: Formal component selection methods used by Rolls-Royce for IPS design [3].

2.2. EAPS Overview

There are three main types of engine air particle separators (EAPS), discussed extensively in Ref. [9], and summarized as:

1. Inertial Particle Separators (IPS), which are usually integrated to the engine inlet and work by forcing air over a hump to radially centrifuge particles, later bifurcating the flow into a dirty scavenge stream and a cleaner core flow stream;
2. Vortex Tube Separators (VTS), which swirl the air and scavenge off centrifuged particles in a separate annular channel at the periphery of the tube, while the inner vortex core of cleaner air passes to the engine;
3. Inlet Barrier Filters (IBF), which consist of several layers of woven wetted cotton media clamped together in a pleated formation, and filter the particulate-laden air that passes through the panel.

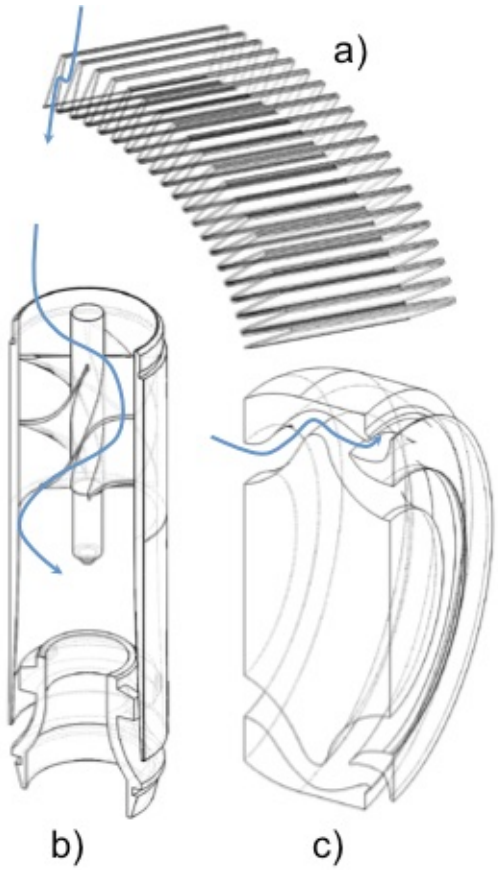

Figure 5: The three EAPS types: a) barrier filter; b) vortex tube; c) inertial particle separator.

Each system removes particles in a different way. A quantitative comparison is given in Ref. [8]. The first two utilize only inertia. Particles of Stokes number less than unity are separated by failing to turn quickly enough with the flow, and crossing streamlines into the scavenge lines. Particles of Stokes number unity and above behave in a ballistic manner, whose inertial forces far outweigh the fluid drag forces upon them. Their route to the scavenge conduit usually entails a series of bounces. The main advantage of inertial type systems over the

barrier filter is the maintainability: their performance does not degrade with time, although vortex tubes are known to get clogged with grass and do occasionally detach from their mounts. However, to achieve separation of the smaller particles relies upon achieving a very quick fluid response time. Vortex tubes achieve their superior separation efficiency over IPS systems by miniaturizing the inertial effect and introducing swirl. However, the cost is a much larger surface area. To minimize pressure loss, the velocity through the tubes is an order of magnitude smaller than that of the IPS, which greatly increases their total frontal cross projected area, thus adding additional drag and weight, in comparison with the IPS system.

The IBF system also requires a large projected area as is evident in Figure 2, in order to minimize pressure loss. To achieve high particle removal efficiency, its fabric filter must also be pleated in formation. In contrast to the inertial systems, the barrier filter collects particles over time which and therefore demands regular maintenance. However, the multiple layers can be tailored to capture a particular particle size, which means that the IBF performs well over a broad range of particle sizes. It can achieve 98% removal efficiency of ISO Coarse test dust, compared with 95% of VTS and 79% of IPS devices [7]. All three generally are generally sized by the requirement to not exceed a maximum pressure loss of in the region of 3% total inlet pressure.

2.3. Hybrid Designs

The idea of a fabric layer optimized to remove a particular size band can be broadened to include other types of particle removal. Since inertial separators can process air at a higher velocity hence lower frontal area, it may make sense to employ them upstream as a pre-filter for the larger particles. Indeed, such 'multi-stage' filtration systems are found often in industrial gas turbine setups [10]. The main difference is that volume and weight are at a premium on aircraft. Any multi-stage filter must be compact enough to fit into the intake plenum or a helicopter.

One such proposal is the hybrid design presented by students at Miami University [11]. The design blended the inertial particle separator concept with the vortex tube, by incorporating an additional obstacle into the central supporting axis of the helix, as shown in Figure 6. Their design managed a peak separation efficiency of 79.3% of MIL-STD-810G test dust, which has a size range of 10-200 microns, although it is not entirely clear what the flow velocity used was.

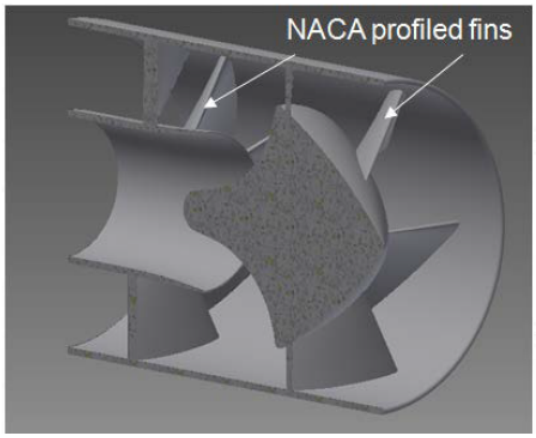

Figure 6: Hybrid EAPS design as presented by University of Miami students [11].

To the author's knowledge, there are no other proposals for hybrid or multi-stage particle separator concepts for helicopter engines. The purpose of the current study is to propose such a concept, that combines the benefits of the inertial and barrier filter systems, to achieve high separation efficiency over a broad range of particle diameters, whilst mitigating the disadvantages of the systems included. A drawing of the system is given in Figure 7.

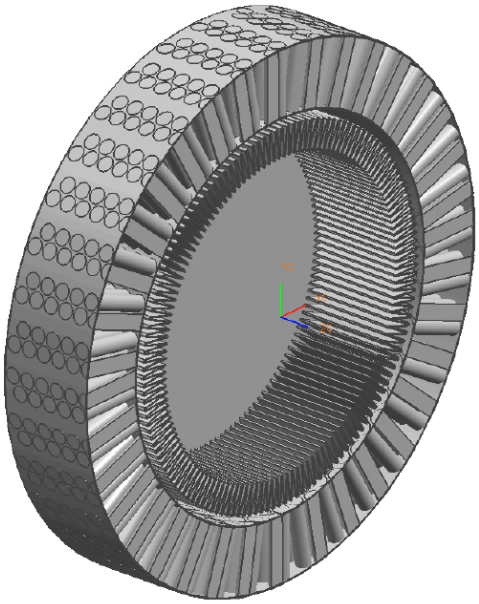

Figure 7: Proposed hybrid EAPS design for this study.

3. THEORY

It is useful to state the fundamental equations that define the performance parameters involved in particle separation.

3.1. Reynolds Number

It has been discussed above that particle separator performance differs depending on the particle diameter. However, the particle size is not the only variable at work. Clearly if the particle enters an inertial type separator at high velocity, it will posses greater inertia. This affects the Reynolds number of particle relative to the flow, and the subsequent drag coefficient that influences the degree of deviation from the streamline. The particle Reynolds number is defined as:

$$Re_p = \frac{\rho_f d_p (u_p - u_f)}{\mu_f} \quad \dots (\ 1 \ )$$

Where u_p is the particle velocity, u_p is the fluid velocity, μ_f is the fluid viscosity, d_p is the particle diameter and ρ_f is the fluid density.

3.2. Particle Drag Coefficient

The drag coefficient C_D varies with particle Reynolds number and can be approximated as follows:

For $Re_p < 1000$

$$C_D = \frac{24}{Re_p}\left(1 + 0.15 {Re_p}^{0.687}\right) \quad \dots (\ 2 \ )$$

For $Re_p > 1000$

$$C_D = 0.44 \quad \dots (\ 3 \ )$$

These approximations are used in particle trajectory calculations to determine the separation efficiency by numerical means.

3.3. Stokes Number

The degree to which a particle deviates from the flow in the presence of a velocity gradient can be assessed using the ratio of response times, or Stokes number. The particle response time is the time taken for a particle, initially in force equilibrium with its carrier, to adjust its trajectory and reach steady state again when the flow changes direction. The characteristic flow time is usually simply defined as a function of the mean flow velocity and a characteristic length such as obstacle diameter:

$$St = \frac{\tau_p}{\tau_f} = \frac{\rho_p {d_p}^2}{18\mu_f}\frac{u_f}{L} \quad \dots (\ 4 \ )$$

Where τ_p is the particle response time, τ_f is the fluid response time, and L is the obstacle length. A Stokes number of much less than unity indicates that the particle will follow the fluid streamlines, whereas a Stokes number much greater than unity implies that the particle will cross fluid streamlines and collide with the obstacle. A Stokes number of around unity may or may not interact with the obstacle, depending on the local streamlines, particle diameter, and perhaps other attractive forces at work close to the obstacle. The particle sizes that inertial separators struggle to remove will have a Stokes number of unity and below.

3.4. Separation Efficiency

The separation efficiency is defined as the ratio of mass of particles removed to mass ingested. Since a portion of the inlet air is scavenged away in inertial-type devices, a correction factor must be employed relating to the scavenge split flow proportion. For example, if 50% of the inlet air is used to scavenge, then 50% of the ingested air was already bound for the scavenge flow. Without the correction factor, the device would appear to have a separation efficiency of 50%, even if no particles are removed from the core portion of the flow. Hence the corrected separation efficiency E' is defined as:

$$E' = \frac{1}{(1-\beta)}(\bar{E} - \beta) \quad \dots (\ 5 \ )$$

Where $\bar{E}$ is the mean separation efficiency over the size distribution in question, and β is the split flow parameter, defined as

$$\beta = \frac{\dot{m}_{06}}{\dot{m}_1 + \dot{m}_{06}} \quad \dots (\ 6 \ )$$

Where $\dot{m}_1$ is the mass flow rate entering the engine, and $\dot{m}_{06}$ is the mass flow rate entering the scavenge line. The mean separation efficiency is defined as:

$$\bar{E} = \frac{\Delta m_{p06}}{\Delta m_{p\infty}} \quad \dots (\ 7 \ )$$

Where Δm_{p06} is the mass of particles collected in the scavenge channel, and $\Delta m_{p\infty}$ is the mass of particles ingested into the particle separator.

3.5. Mass Flow Rate

Each particle separator must ensure that sufficient mass flow of air reaches the engine. Some separators function better with a low face velocity.

This can be calculated by applying the mass continuity equation for incompressible flow:

$$\dot{m} = \rho_f u_f A_{05} \quad \text{... (8)}$$

Where A_{05} is the particle separator total projected area, with subscript 05 to denote the engine station number (with 1 being the engine inlet). Note: for inertial type separators that utilize scavenge, the mass flow rate is a summation of the core mass flow rate demanded by the engine, and the mass flow rate required by the scavenge system.

4. METHODOLOGY

In the current work, we propose a methodology to rank engine air particle separator designs and use it to assess the performance of a new hybrid design for a hypothetical set of requirements.

4.1. Figure of Merit

To assess particle separators against each other, we derive a mean Figure of Merit that encompasses many of the performance parameters:

$$\overline{FoM} = \bar{E}\left(\frac{A_1}{A_{05}}\right)\left(\frac{p_{T,1}}{p_{T,05}}\right)\left(1 - \frac{P_{06}}{P_{SP}}\right) \quad \text{... (9)}$$

Where A_1 is the engine inlet area, A_{05} is the EAPS projected area, $p_{T,1}$ is the total pressure at the engine inlet, $p_{T,05}$ is the total pressure at the EAPS inlet, P_{SP} is the shaft power delivered by the engine, and P_{06} is the power required by the scavenge pump or ejector. Each parameter in Equation 9 except the area ratio is a function of the operating point. A mean Figure of Merit close to unity whilst ingesting the target contaminant dust composition at the engine design point, is the optimum particle separator.

4.2. Separation Efficiency

The separation efficiency for each particle separator is not only a function of the particle diameter; the Stokes number is a more appropriate independent variable, although it is unique to the separator in question. Writing in terms of Stokes number allows the efficiency of separation to include the influence of particle *and* fluid inertia, rather than just particle size as is usually the case when separation efficiency is quoted. The grade efficiency is the separation efficiency as a function of Stokes number:

$$\eta_{EAPS} = f(St) \quad \text{... (10)}$$

The mean efficiency is found when there is a mass-weighted distribution of Stokes number to apply the grade efficiency. The mean efficiency is therefore:

$$\bar{E} = \sum_{i=1}^{N_p} {m_i}^* E_{EAPS}(St_i) \quad \text{...(11)}$$

Where the subscript i refers to a discrete size band converted into a Stokes number, St_i, by Equation 4, and ${m_i}^*$ is the fraction of total mass occupied by that size band. The mid-size diameter of the size band is commonly used as the characteristic diamater to determine the representative Stokes number. The Stokes number is largely interchangeable with particle diameter, which is the dominant parameter. Indeed, displaying as a function of particle diameter may be more meaningful. However, since a device's ability to separate depends also upon the flow condition, it is appropriate to display as a function of Stokes number. Inclusion of the mass fraction allows the proportion of the total particulate mass separated to be found through summation of the mass separated at each distinct Stokes number.

The grade efficiency function is unique to the separator. Here we present some analytical and empirical formulas to predict grade efficiency as a function of Stokes number and, where possible, device geometry.

4.2.1 Inertial Particle Separators

Inertial particle separators rely quite heavily on particle bounce to achieve high separation efficiency of ballistic particles. The influence of wall geometry is great, which makes derivation of an anlytical model quite difficult. Experiments by Loth et al. [12] however have shown that the grade efficiency can be predicted to reasonable accuracy for particles greater than 20 microns using the following formula:

$$\eta_{IPS} = (1 - \beta)\frac{St_H}{St_H + C} + \beta \quad \text{... (12)}$$

The constant C is found empirically, and is unique to the geometry. Loth et al. tested three geometries with differing outer wall contours [12]. The value of C for the best-performing geometry was found to be 0.046. The equation for Stokes number is as presented in Equation 4, with the characteristic length being the distance from IPS inlet to engine inlet, and the characteristic velocity being the inlet velocity.

4.2.2 Vortex Tube Separators

The theory for vortex tube separators assumes purely non-ballistic separation. That is, the particle is swirled within the vortex tube, which imparts a radial acceleration to the particle. The particle radial motion is assumed to occur in steady state terminal velocity, with the drag force induced by the relative velocity balanced by the radial force field. The separation zone within the vortex tube, depicted in Figure 8, is where the particle has time to reach the outer annular region of flow that is scavenged away.

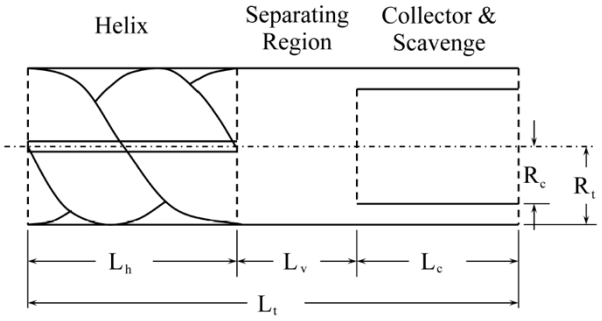

Figure 8: Anatomy of the vortex tube separator.

The grade efficiency was derived analytically by Ramachandran [13] and is adopted for helicopter VTS as:

$$\eta_{VTS} = (1-\beta)\left[1 - \mathrm{e}^{\left(\frac{-8\pi Q_f \tau_p L_v}{{R_c}^2 P^2}\right)}\right] + \beta \qquad \text{... (13)}$$

Where Q_f is the tube volume flow rate, R_c is the collecting tube radius, L_v is the length of the separating region, and P is the pitch of the helix, which determines the turning rate of the swirl. By defining a Stokes number for vortex tubes as:

$$St_{VTS} = \frac{\tau_p}{\tau_f} = \frac{\rho_p {d_p}^2}{18\mu_f}\frac{L_v u_f}{P^2} \qquad \text{... (14)}$$

the grade efficiency can be re-written as

$$\eta_{VTS} = (1-\beta)\left[1 - \mathrm{e}^{\left(\frac{-8\pi^2}{(1-\beta)} St_{VTS}\right)}\right] + \beta \qquad \text{... (15)}$$

The inclusion of the split flow parameter β in the exponent of the exponential caters to the fact that the efficiency of separation is affected by the ratio of collector radius to outer tube radius.

4.2.3 Inlet Barrier Filters

Filters capture particles using a web of fibres. There are many capture mechanisms at work, a discussion of which can be found in Ref. [7]. Inlet barrier filters typically contain a number of layers, which may be tailored to capture particles of a certain Stokes number. The layer efficiency is determined by parameters such as inter-fibre spacing, packing fraction, and flow velocity. The grade efficiency of an IBF is given by:

$$\eta_{IBF} = 1 - e^{\left(-\frac{4\alpha Z_F \eta_E}{\pi(1-\alpha)d_f}\right)} \qquad \text{... (16)}$$

Where α is the packing fraction of the filter (the proportion of filter volume made up of fibres), Z_F is the thickness or depth of the filter, η_E is the collection efficiency of a single fibre in the filter medium, and d_f is the fibre diameter. The overall efficiency is seen to improve with increasing packing fraction and decreasing fibre diameter. The influence of Stokes number is buried within the finer definition of single fibre efficiency, and will not be elaborated here; for more details see Bojdo [7]. The characteristic length in the formula for Stokes number is the fibre diameter, and the characteristic velocity is the bulk flow velocity through the medium. The packing fraction actually increases over time due to the collection of particles within the filter, however this will not be considered in the current study. The negative impact of particle accumulation is of course a temporally increasing pressure loss.

4.3. Core Pressure Ratio

Total pressure is lost across a particle separator to numerous sinks. Firstly there is the loss to work against friction, which is common to all types of separator. Then there is the dynamic pressure necessary to actuate the change in flow direction such as the swirl in vortex tubes. Finally, any large areas of flow separation need to be accounted for. Models to predict these losses are unique to each separator type, and are derived in other works [7]. They are restated here for brevity.

4.3.1 Inertia-type Separators

Research in the field of inertial particle separators has identified a flow feature unique to inertial particle separators: a separation zone on the outer wall of the entry to the scavenge flow line, see Figure 9. This complicates deriving an analytical solution for the pressure drop of an IPS. Furthermore, in two independent studies on IPS aerodynamics [14], [15], the flow is seen to accelerate at the peak of the hump, which means the frictional losses will vary along the wall.

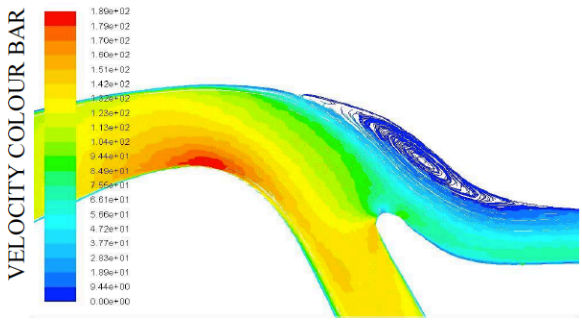

Figure 9: Velocity magnitude plot and fluid streamlines of an Inertial Particle Separator.

In vortex tubes, the air is swirled by a vortex generator that is fixed to the walls of the tube. A separated flow area exists in these, too, just aft of the generator, as depicted in Figure 10.

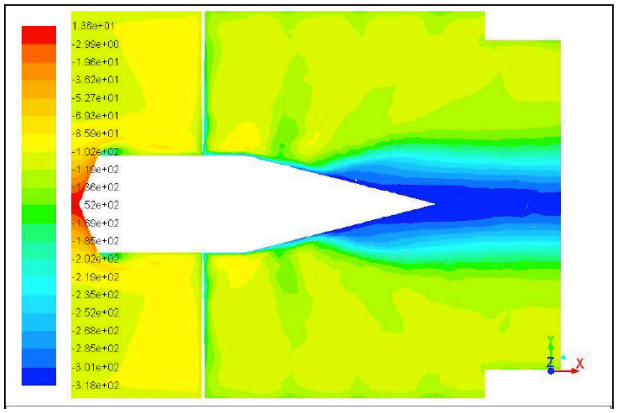

Figure 10: Contour plot of total pressure in a Vortex Tube Separator from a RANS simulation. The blue region indicates separated flow.

In a first order analytical model, these effects are ignored. Instead we apply the Darcy-Weisbach equation to estimate the frictional losses through a cylinder, of the form:

$$\Delta p_{fric} = \frac{f \rho_f L_{path} {u_{f,ave}}^2}{2 D_H} \qquad \ldots(\quad 17 \quad)$$

Where L_{path} is the average length of path of gas through the particle annular particle separator, V_{avg} is the average velocity of the gas, and D_H is the hydraulic diameter. The friction factor f is defined as:

$$\sqrt{\frac{1}{f}} = -1.8 \log_{10}\left[\frac{6.9}{Re_f} + \left(\frac{\epsilon/D}{3.7}\right)^{1.11}\right] \qquad \ldots(\quad 18 \quad)$$

Where ϵ/D is the relative roughness of the wall and Re is the Reynolds number of the cylinder, assuming hydraulic diameter as a reference length and average velocity $u_{f,ave}$ as a reference velocity.

The dynamic pressure is calculated simply as:

$$\Delta p_{dyn} = \rho_f \left(\frac{{u_{f,ave}}^2 - {u_{f05}}^2}{2}\right) \qquad \ldots(\quad 19 \quad)$$

Where u_{f05} is the velocity at the entry to the inertial type separator.

4.3.2 Inlet Barrier Filters

The pressure drop across a barrier filter is a function of the porous medium properties and the face velocity:

$$\Delta p_{filt} = \Delta Z_F \left(C_1 \mu_f u_f + \frac{1}{2} C_2 \rho_f {u_f}^2\right) \qquad \ldots(\quad 20 \quad)$$

Where ΔZ_F is the filter thickness and C_1 and C_2 are the viscous and inertial resistance coefficients. These coefficients are determined experimentally. If the filter is pleated, the coefficients can be minimized for a given flow rate by optimizing the pleat geometry (see Ref. [7]). Pleating a filter allows a greater *cloth-to-air ratio,* which reduces the face velocity and therefore pressure loss across the medium. However, the pleat channels become a new source of pressure loss as a boundary layer sets up at the porous interface.

4.3.3 Overall Pressure Ratio

The overall pressure ratio is simply calculated as a summation of the respective contributory sources, normalized with the dynamic pressure at the engine inlet (post-separator):

$$\left(\frac{p_{T,1}}{p_{T,05}}\right) = 1 - \frac{\Delta p_{EAPS}}{q_1} \qquad \ldots(\quad 21 \quad)$$

Where Δp_{EAPS} is the total pressure loss for the particle separator in question.

4.4. Auxiliary Power Required

Auxiliary power refers to the additional power required to operate the particle separator over the power required by the engine to overcome the pressure loss of the core airflow. The two inertial systems require an extraction system to exhaust the dirty air stream. The power required must be large enough to pull the required mass flow and overcome pressure losses and flow separation in the channel. The vortex tube separator scavenge

system is packed in tightly; modeling the pressure loss is made difficult by the fact that each solution may have a radically different geometry to another solution. In the absence of a better model, we focus on the pressure loss due to the frictional losses from the duct wall, using the Darcy-Weisbach equation in Equation 12. The power required can then be determined from the energy equation and normalized with the engine power:

$$1 - \frac{P_{06}}{P_1} = 1 - \frac{\dot{m}_1 \beta \Delta p_{scav}}{(1-\beta) q_1 \rho_f} \qquad \ldots(\quad 23 \quad)$$

Where Δp_{scav} is the pressure loss in the scavenge channel, which is calculated via Equation 12. We normalize with the power required by the engine to achieve the desired mass flow rate at the engine inlet (post-separator). Note: it is assumed that the mass loading of particles in the scavenge flow is small enough to have negligible effect on the dirty gas density. (For example, a typical brownout concentration of 1.225 g/m^3 equated to a mass loading of 10^{-4} kg/kg, or 1 gram of dust for every kilogram of air). Equation 18 can be safely applied to barrier filters, since they require no scavenge airflow, hence $\beta = 0$.

5. RESULTS & DISCUSSION

We begin with a brief discussion of each EAPS type's performance, and then demonstrate the performance enhancement that could be achieved with a hybrid EAPS design.

5.1. Vortex Tube Performance

Figure 11 shows the separation efficiency as a function Stokes number as defined in Equation 14. Of note is the tendency towards 100% efficiency at Stokes numbers of greater than 0.05, which is perhaps a little lower than convention dictates. There is also no disparity between the lines, which is expected since the only two parameters that were varied are featured in the Stokes number equation. This result is expected since the solution is purely analytical. This demonstrates that the separation efficiency of a vortex tube can be improved by reducing the helix pitch and by increasing the separating zone. The effect of increased scavenge flow was not investigated, however interestingly each geometry exhibited a different pressure loss, with the 10 m/s faring worst. The benefit of increasing axial velocity is that fewer tubes are required to meet the engine mass flow demand. This is a design trade-off.

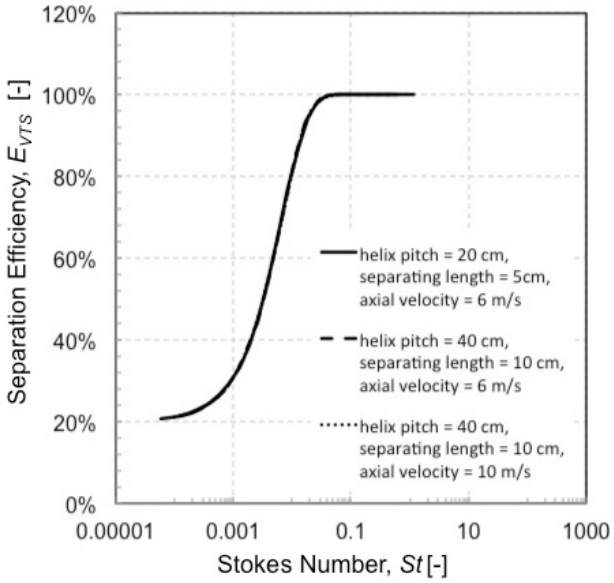

Figure 11: Effect of Stokes number of separation efficiency of a vortex tube separator.

5.2. Inlet Barrier Filter Performance

The separation efficiency of a barrier filter for three combinations of two design parameters is shown in Figure 12 and Figure 13. We assume that the filtration velocity is met with a balance of pleating and sizing of the filter panel to meet the engine mass flow demand without excessive projected area (see Ref. [7]).

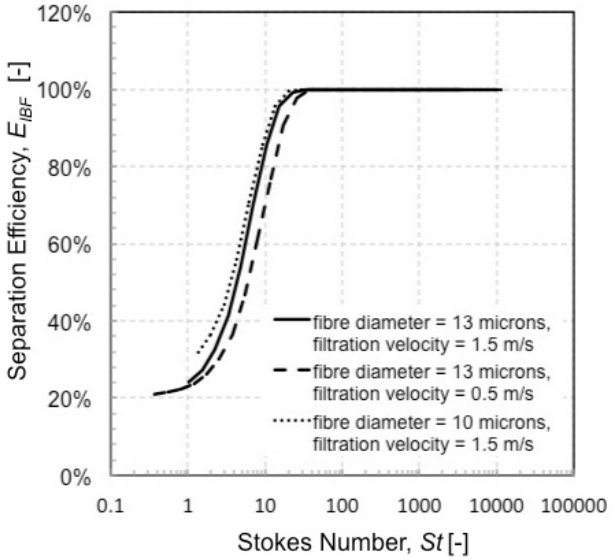

Figure 12: Effect of Stokes number, fibre diameter and filtration velocity of separation efficiency of an inlet barrier filter.

In Figure 12, the separation efficiency for a given Stokes number is seen to improve slightly with decreasing fibre diameter and increasing face velocity, all other variables (such as packing fraction) held constant. Single fibre theory dictates that the larger the cylinder radius, the slower is the turning of the air, hence the more time the particle has to *respond* to the flow. Similarly, though, if the particle approaches the cylinder at a high velocity, its increased inertia will result in a greater deviation from the flow when encountering an obstacle. These benefits must again be traded off with the increased pressure loss to friction in both cases.

Interestingly, the lines are not exactly superimposed upon one another as in the case of the vortex tube, despite the Stokes number requiring velocity and fibre diameter to define the fluid response time. Furthermore, the efficiency begins to increase towards 100% at Stokes numbers almost two orders of magnitude greater than the vortex tubes. Conventional use of Stokes number assumes particles to become *ballistic* at Stokes numbers approaching unity. The definition of Stokes number for IBF may there need to be revisited to improve its use as a first order estimate of capture efficiency.

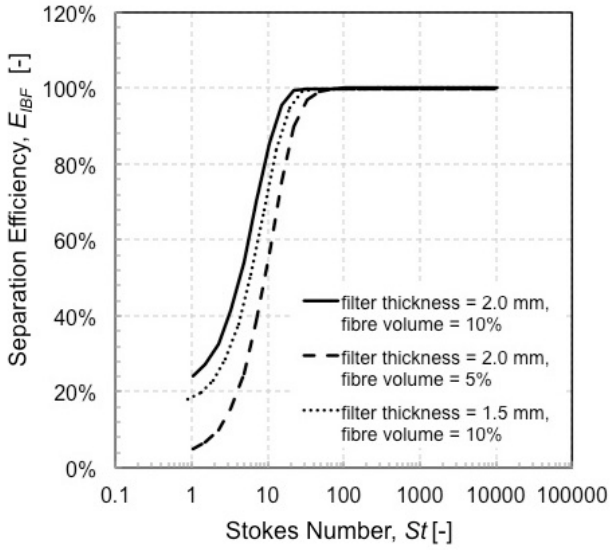

Figure 13: Effect of Stokes number, packing fraction and filter thickness on separation efficiency of an inlet barrier filter.

To emphasise this point, Figure 13 shows the effect of changing the packing fraction (proportion of filter volume constituted by fibres) and filter thickness on separation efficiency, which is considerable. Again, since the purpose of Stokes number is to find a universal parameter that can be used as a first estimate of likelihood of capture, the presence of this discrepancy perhaps justifies looking at away to include these other two geometrical parameters in the definition. Not least due to the fact that the packing fraction increases over time due to clogging, and the thickness may increases due to accumulation of a cake layer. Incidentally, whilst clogging improves the filter's collection efficiency further, the pressure drop can increase by five times, to the detriment of engine performance.

5.3. Inertial Particle Separator Performance

Inertial particle separators are less amenable to analytical methods owing to the numerous geometrical parameters that define the scavenge channel, hump, and splitter, and the added variable of scavenge mass flow. Nevertheless, as discussed above, empirical formulas have been derived in the literature. We present in Figure 14 the separation efficiency of two geometries, OSG-1 and OSG-2, which have values of C of 0.046 and 0.111 respectively. We also show the effect of varying the split flow parameter, β.

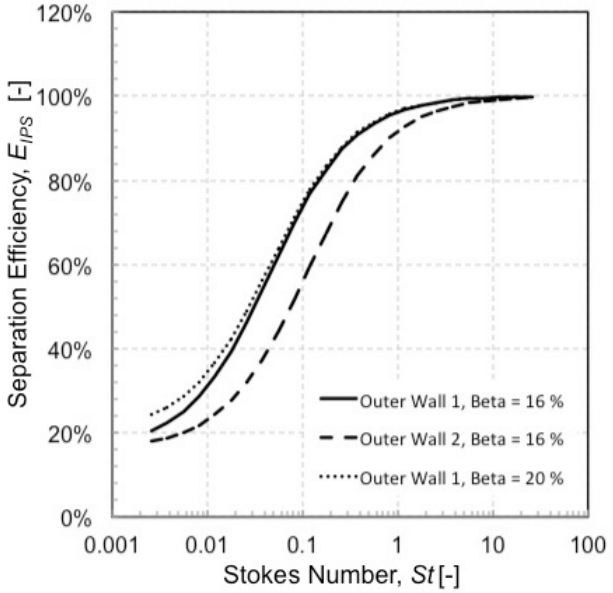

Figure 14: Effect of Stokes number, outer wall geometry design, and scavange mass flow proportion on separation efficiency of an inertial particle separator.

The graph shows that the influence of scavenge mass flow rate is prevalent only at low Stokes numbers, and to a limited degree. At such Stokes numbers, the particles are too small to behave

ballistically, yet still possess enough inertia to deviate from fluid streamlines. This suggests that the scavenge channel's role is not to 'suck' particles from the core flow, but merely to act as a *deposit bin* for those particles that bounce out of the core air flow. In this case the value of scavenge mass flow irrelevant, provided there is a location for particles to bounce into, and that the scavenge mass flow is not so small that the engine core flow will actually suck a greater concentration of particles than was already present in the core air flow.

The effect of outer wall geometry on the other hand is seen to be much more influential on separation efficiency. In this case, the geometry of OSG-2 featured a much wider inlet to the scavenge channel than OSg-1, which resulted in a localized separation zone on the upper wall at the scavenge inlet. It is thought that this influenced the flow path to such an extent that some of the particles that were initially destined for the scavenge channel were re-diverted towards the core engine airflow.

Due to the high flow speeds in an IPS, the pressure lost to frictions with the duct walls is much greater than the VTS. The benefit of this, though, is a much more compact, low drag and low weight solution. Note: we have excluded these cost functions from our Figure of Merit due to difficulties in obtaining relevant data.

5.4. Figure of Merit all three EAPS

To allow a comparison of the three devices, we construct a hypothetical situation of designing a new EAPS system to protect against the so-called *reactive sands* that contain low-melting point minerals that can deposit on internal engine surfaces and restrict the flow capacity. A dust referred to as "AFRL02" was created by the US Air Force Research Lab to more realistically reflect the dust type found in and around the Persian gulf, than the standard ISO tests dusts that are used in engine sand and dust susceptibility tests. For comparison, we also apply the methodology to the industry standard ISO Coarse test dust. A cumulative mass distribution curve is present in Figure 15 for comparison.

We then assume we are designing an engine protection device for a large turboshaft engine with a mass flow of 12.5 kg/s and an engine inlet velocity (v_1) of 100 m/s. For the inertial particle separator, we have borrowed empirical constants from Ref. [12]. The inlet conditions on entry to each particle separator are ISA Standard Day.

The separation efficiency curves of Figures 11 to 14 become of practical use when applied to a mass fraction distribution of a given dust. The curves in Figure 15 can also be written as probability density function, in which the abscissa is discretized into size 'bins'. The particles in each size bin are weighed and divided by the total weight in the sample to determine their mass fraction. Each size bin also has a characteristic diameter, usually its mid-size, which can be used as a representative diameter to find the corresponding separation efficiency, thence the percentage of that particular size band that is removed by the EAPS device in question. The overall mass-weighted separation efficiency is then simply a summation of the separated mass fractions of the whole size distribution, as described by Equation 11.

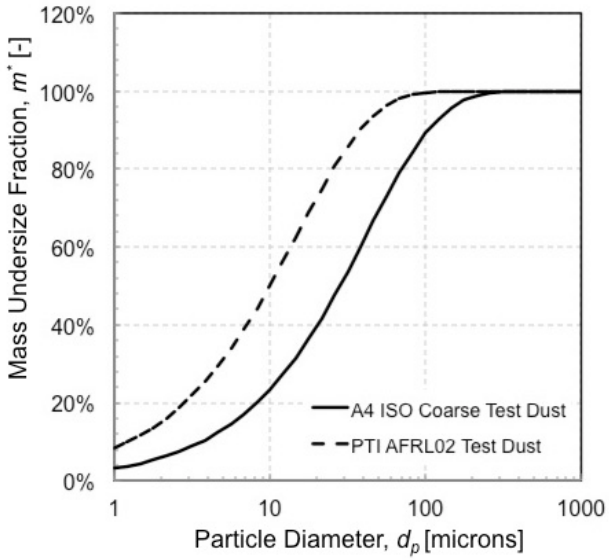

Figure 15: Cumulative mass distribution curves for AFRL02 test dust, and A4 ISO Coarse test dust.

The overall separation efficiency of each device when filtering two test dusts are shown in Table 1.

	Separation Efficiency	
	ARFL02	**ISO Coarse**
Vortex Tubes	72.5%	95.1%
Barrier Filter	87.7%	95.7%
Inertial Separator	75.5%	88.7%

Table 1: Mass-weighted mean separation efficiency of each partice separator type for AFRL 02 test dust and A4 ISO Coarse test dust. The latter is an industry standard.

It is notable that in each case, the inlet barrier filter performs best, although the values are of a comparable magnitude. Perhaps more expectedly the overall efficiencies are lower for AFRL02, which is a much finer test dust. It also happens to contain a higher proportion of clay and feldspar minerals that have a lower melting point than quartz hence a greater likelihood of becoming molten and depositing on internal engine surfaces. This highlights the importance of qualifying particle separators with an appropriate test dust: the industry standard approach (as stated in manufacturers' brochures) is to quote the separation efficiency for A4 ISO Coarse test dust, which is a demonstrably better performance than is achievable in a realistic operation environment.

It was discussed that there is often a trade-off between achieving high separation efficiency and low pressure loss. Furthermore, some EAPS devices require additional power to fluidise the scavenge channel. The Figure of Merit is a useful metric to assess the efficacy of the three devices applies to this particular case. Figure 16 shows the FoM as a function of the particle response time for each device. We have chosen to use response time to overcome the fact that the characteristic fluid response time is quite different for each device. The particle response time for a size distribution of constant density is proportional to the square particle diameter. Its use is preferred over particle diameter because dust distributions are seldom of constant density and vary across the size distribution; we use constant density here for simplicity.

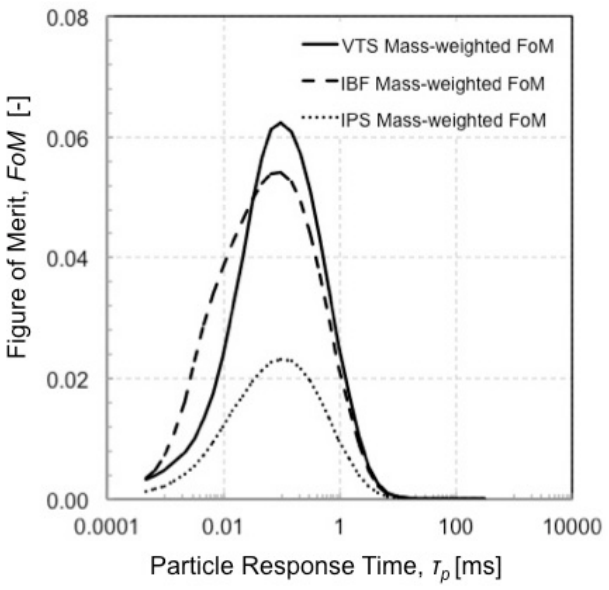

Figure 16: Variation of mass-weighted Figure of Merit across a particle response time distribution of AFRL 02.

The value of Figure of Merit is mass weighted; the larger the proportion of mass occupied by a particular size band, the larger the mass that is separated. While this does not permit a useful comparison between size bands, since the initial particle size distribution is identical for each particle separator type. Therefore mass-weighted Figure of Merit affords an insight into how well each particle separator performs across the distribution. From Figure 16, we can see that the vortex tube achieves the best Figure of Merit of all deices at the most abundant particle response time, but is second best to the IBF at lower particle response times. This is reflective of the fact that at low Stokes numbers, the vortex tubes still rely on inertia to persuade particles into the scavenge flow to be separated. Yet achieving a comparable fluid response time such that the smallest particles cross fluid streamlines becomes increasingly difficult at small particle size, below 10 microns. The IBF achieves this with equivalent-sized fibre diameters; in the region of Figure 16 in which IBF FoM exceeds VTS, the pressure loss must also be 'worth it'. IPS has notably inferior performance in comparison to the other two, mainly due to the much greater pressure loss.

	Figure of Merit	
	ARFL02	**ISO Coarse**
Vortex Tubes	71.8%	86.9%
Barrier Filter	75.0%	81.3%
Inertial Separator	29.0%	34.1%

Table 2: Mass-weighted mean Figure of Merit of each particle separator type for AFRL02 and A4 ISO Coarse test dust.

The consequence of the finding from Figure 16 is that one may wish to utilise the qualities of two types of technology to remove more material for no additional cost (and perhaps even a saving). The mass weighted Figure of Merit helps by allowing one to assess different particle separator concepts for a particular target dust distribution. In a similar way to the overall separation efficiency, we can determine the mass-weighted Figure of Merit for the whole dust distribution. These are compared for each device in Table 2. It is interesting to note that the vortex tubes are now the preferred choice for filtering A4 ISO Coarse test dust, when pressure loss and scavenge power costs are taken into

account. However the barrier filter concept, despite displaying a lower peak FoM value in Figure 16, achieves a higher overall FoM due to decent performance over a wider range of particle sizes.

It is worth reiterating at this point that we have not included in the Figure of Merit the favorable feature of compactness that an IPS has over its counterparts. Both VTS and IBF need to be mounted externally on the airframe to ensure that there is enough filtration area to reduce the face velocity to a level that does not incur a sever pressure loss. We aim to account for this in future iterations. Furthermore, the individual components of the Figure of Merit may impact on the engine in differing amounts: a percentage point loss of pressure will probably incur a much greater loss off engine performance than a percentage point loss of separation efficiency. Therefore we envisage these cost functions to be weighted in future, to reflect overall effect on the engine's life cycle. This may require customer input, and is a topic of future work.

5.5. Hybrid EAPS Performance

The results of the Figure of Merit study suggest that one particle separator may be more appropriate than another, for a mass fraction distribution of particle diameters. We propose, therefore, a new particle separator that utlises VTS technology for the larger particle fraction of the target dust, and utilizes IBF technology for the smaller size fractions. The VTS effectively acts as a pre-filter, allowing more time an attention for the IBF to focus on filtering the smallest particles before clogging reaches and unacceptable level. A drawing of the proposed design is presented in Figure 7.

The result is shown in Figure 17, which shows the change in particle size distribution (PSD) of the original AFRL 02 test dust when filtered solely by VTS, solely by IBF, and lastly the particle size distribution when filtered a VTS stage followed by an IBF stage. One can see the benefit of such an approach: the final PSD covers a smaller range of particles with a lower peak mass fraction, indicating that this device is capable of achieving a higher overall separation efficiency. Indeed, the efficiency is calculated to be 90.6%.

The remaining challenge is to optimize the design of the IBF for a reduced particle size distribution as if the original dust has been filtered by the VTS. To compare the hybrid approach, we take a mass-weighted average of the overall mass-weighted FoM over the two stages, and find a value of 60.51%. This loss of FoM may be acceptable in the context of engine longevity; investigation of this, and the implementation of weightings in the Figure of Merit remains part of our ongoing work.

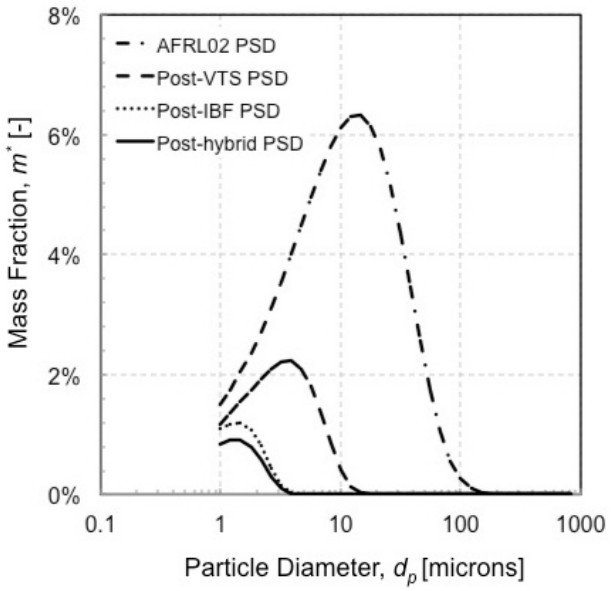

Figure 17: Changes to the particle size distrobution of AFRL 02 when filtered by different particle separator concepts.

6. CONCLUSIONS

1. An integrated approach to particle separator selection is required in order to design the optimal system, largely due to the competing forces of pressure loss and separation efficiency.
2. The target particle size distribution is very important in concept selection. Existing dependence on standard dusts to test and certify particle separators may result in the ingestion of material with a higher potential to deposit, thus undermining the lifing models that are constructed using engine test data.
3. A new *Figure of* Merit for EAPS design was shown to benefit concept choice: vortex tubes were found to exhibit a better Figure of Merit than barrier filters and inertial particle separators in the removal of AC Coarse Test Dust.
4. A hybrid particle separator, containing a vortex tube pre-filter followed by barrier filter second stage, was shown to achieve superior separation efficiency, albeit at a reduced overall Figure of Merit.

7. REFERENCES

[1] P. Stallard, “Helicopter Engine Protection,” *Perfusion*, vol. 1997, no. 12, pp. 263–267, Jul. 1997.

[2] J. L. Smialek, F. A. Archer, and R. G. Garlick, “Turbine airfoil degradation in the persian gulf war,” *JOM*, vol. 46, no. 12, pp. 39–41, Dec. 1994.

[3] D. L. Mann and G. D. Warnes, “Future Directions in Helicopter Engine Protection System Configuration,” in *Agard Conference Proceedings Agard Cp*, 1994, pp. 4–4.

[4] A. Hamed, W. Tabakoff, and R. Wenglarz, “Erosion and deposition in turbomachinery,” *J. Propuls. Power*, vol. 22, no. 2, pp. 350–360, 2006.

[5] “Fatal MV-22 crash in Hawaii linked to excessive debris ingestion.” [Online]. Available: https://www.flightglobal.com/news/articles/fatal-mv-22-crash-in-hawaii-linked-to-excessive-debr-419484/. [Accessed: 24-Sep-2016].

[6] V. Hwa, “Test And Evaluation Of An Inlet Barrier Filter To Increase Engine Time-on-wing For The Bell Boeing V-22 Osprey Tiltrotor,” Jul. 2015.

[7] N. Bojdo, “Rotorcraft Engine Air Particle Separation,” PhD Thesis, University of Manchester, 2012.

[8] N. Bojdo and A. Filippone, “A Comparative Study of Helicopter Engine Air Particle Separation Technologies,” in *Proceedings of the 38th European Rotorcraft Forum*, Amsterdam, Netherlands, 2012.

[9] A. Filippone and N. Bojdo, “Turboshaft engine air particle separation,” *Prog. Aerosp. Sci.*, vol. 46, no. 5–6, pp. 224–245, Jul. 2010.

[10] M. Wilcox, R. Baldwin, A. Garcia-Hernandez, and K. Brun, “Guideline for gas turbine inlet air filtration systems,” *Gas Mach. Res. Counc. Dallas TX*, 2010.

[11] A. D. Cozier, K. E. Harned, M. A. Riley, B. H. Raabe, A. D. Sommers, and H. A. Pierson, “Additive Manufacturing in the Design of an Engine Air Particle Separator,” in *ASME 2015 International Mechanical Engineering Congress and Exposition*, 2015, p. V001T01A037–V001T01A037.

[12] D. Barone, E. Loth, and P. Snyder, “Influence of particle size on inertial particle separator efficiency,” *Powder Technol.*, vol. 318, pp. 177–185, Aug. 2017.

[13] O. Ramachandran, P. C. Raynor, and D. Leith, “Collection efficiency and pressure drop for a rotary-flow cyclone,” *Filtr. Sep.*, vol. 31, no. 6, p. 631–636,630, 1994.

[14] D. Barone, E. Loth, and P. Snyder, “Fluid Dynamics of an Inertial Particle Separator,” 2014.

[15] M. Taslim, A. Khanicheh, and S. Spring, “A Numerical Study of Sand Separation Applicable to Engine Inlet Particle Separator Systems,” *J. Am. Helicopter Soc.*, vol. 54, no. 4, pp. 42001–42001, 2009.